Available online at www.sciencedirect.com
SCIENCE DIRECT®
Journal of Organometallic Chemistry 690 (2005) 629–639
Journal of Organometallic Chemistry
www.elsevier.com/locate/jorganchem

Synthetic, structural, spectroscopic, and electrochemical studies of mixed sandwich Rh(III) and Ir(III) complexes involving Cp* and tridentate macrocycles

Gregory J. Grant [a,*], John P. Lee [a], Monte L. Helm [a], Donald G. VanDerveer [b], William T. Pennington [b], Jeffrey L. Harris [b], Larry F. Mehne [c], David W. Klinger [c]

[a] *Department of Chemistry, The University of Tennessee at Chattanooga, USA*
[b] *Department of Chemistry, Clemson University, USA*
[c] *Department of Chemistry, Covenant College, USA*

Received 26 August 2004; accepted 6 October 2004

Abstract

The syntheses, structures, spectroscopy, and electrochemistry for six Ir(III) and Rh(III) mixed sandwich mononuclear complexes involving tridentate macrocycles and pentamethylcyclopentadienide (Cp*) are reported. The complexes are readily prepared by direct ligand substitution reactions from the dichloro bridged binuclear complexes, $[\{M(Cp^*)(Cl)_2\}_2]$. All complexes have the general formula $[M(L)(Cp^*)]X_2$ (M = Ir(III) or Rh(III), L = macrocycle, $X = PF_6^-$ or Cl^-) and exhibit a distorted octahedral structure involving three donor atoms from the macrocycle and the facially coordinating carbocyclic Cp* ligand. The complex cations include: $[Rh(\eta^5\text{-}Cp^*)(9S3)]^{2+}$ (**1**), $[Rh(\eta^5\text{-}Cp^*)(9N3)]^{2+}$ (**2**), $[Rh(\eta^5\text{-}Cp^*)(10S3)]^{2+}$ (**3**), $[Ir(\eta^5\text{-}Cp^*)(9S3)]^{2+}$ (**4**), $[Ir(\eta^5\text{-}Cp^*)(9N3)]^{2+}$ (**5**), and $[Ir(\eta^5\text{-}Cp^*)(10S3)]^{2+}$ (**6**), where 9S3 = 1,4,7-trithiacyclononane, 9N3 = 1,4,7-triazacyclononane, and 10S3 = 1,4,7-trithiacyclodecane. The structures for all six complexes are supported by ^1H and $^{13}C\{^1H\}$ NMR spectroscopy, and five complexes are also characterized by single-crystal X-ray crystallography (complexes **1**–**5**). The ^1H NMR splittings between the two sets of methylene protons for both the Rh(III) and Ir(III) 9S3 complexes are much larger (0.4 vs. 0.2 ppm) compared to those in the two 9N3 complexes. Similarly, the $^{13}C\{^1H\}$ NMR spectra in all four thioether complexes show that the ring carbons in the Cp* ligand are shifted by over 10 ppm downfield compared to the azacrown complexes. The electrochemistry of the complexes is surprisingly invariable and is dominated by a single irreversible metal-centered reduction near −1.2 V vs. Fc/Fc^+.

Keywords: 1,4,7-Trithiacyclononane; Rhodium complexes; Iridium complexes; Mixed sandwich complexes; Macrocyclic ligands; Pentamethylcyclopentadienide complexes

1. Introduction

For the past two decades, the coordination chemistry of the tridentate macrocycles 1,4,7-triazacyclononane (9N3) and 1,4,7-trithiacyclononane (9S3) has been an important focus of the inorganic community (see structures below) [1–3]. More recent work with these types of macrocyclic ligands includes the examination of their organometallic chemistry [4–14]. The two macrocycles can be compared to η^5-cyclopentadienide and pentamethylcyclopentadienide (Cp and Cp*), η^6-arene, and κ^3-$HB(pz)_3$ (pz = pyrazol-1-yl) (Tp) ligands in that all are six electron donors which occupy three facially coordinating sites. Mixed sandwich compounds with the general formula $[M(\eta^5\text{-}Cp)(L)]^+$ (M = Fe, Ru; L = 9S3, 10S3) (1,4,7-trithiacyclodecane) and $[M(\eta^6\text{-arene})(L)]^{2+}$

* Corresponding author. Tel.: +42 34 254 143; fax: +42 34 255 234.
E-mail address: Greg-Grant@utc.edu (G.J. Grant).

0022-328X/$ - see front matter © 2004 Elsevier B.V. All rights reserved.
doi:10.1016/j.jorganchem.2004.10.010

(M = Ru; L = 9S3, 10S3, 11S3) have now been prepared by several research groups [15–18].

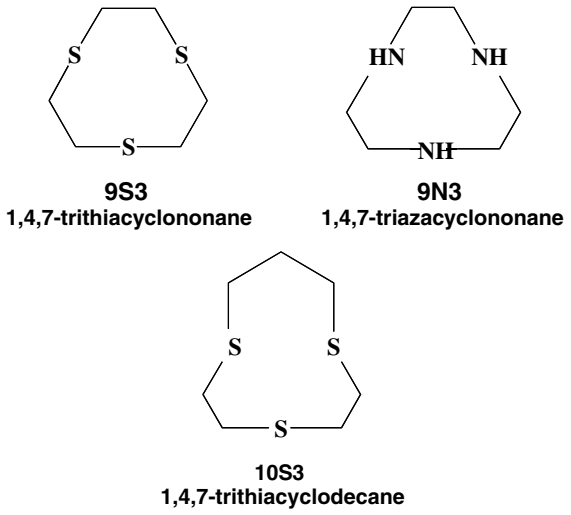

The mixed sandwich complexes possess heteroleptic ligand environments which are intermediate between the corresponding metallocenes and hexakis(thioether) complexes, and, accordingly, exhibit structural, spectroscopic, and electrochemical properties which are intermediate between the two types of homoleptic sandwich complexes. Goh and co-workers [19] have recently extended this chemistry to include the strongly electron-donating Cp* ligand with the synthesis and characterization of the mixed sandwich complex [Ru(η^5-Cp*)(9S3)](PF_6). Our current work further expands the examination of mixed sandwich complexes containing Cp* and the three tridentate macrocycles to include the two Group 9 metal ions, Rh(III) and Ir(III).

There are a few reports involving Rh(III) and Ir(III) Cp* complexes with amine and thioether ligands, but complexes involving macrocyclic ligands are more limited [20–22]. Interest in Rh(III) and Ir(III) complexes with carbocyclic ligands such as Cp* arises from their important role as catalysts in C–H bond activation in aliphatic and aromatic hydrocarbons [23,24]. There have been a few reports of Rh(III) complexes with thiacrowns [9,25–29], but only two reports of complexes containing carbocyclic ligands [22,30]. As noted recently by Sheldrick, reports of second and third row transition metal complexes with 9N3 are surprisingly scarce [31,32]. This is especially true for Ir(III) complexes involving any of these three macrocycles [33,34]. The macrocycle 1,4,7-triazacyclononane (9N3) is both a better σ-donor ligand and poorer π-acceptor than 9S3. Since the σ/π donor/acceptor characteristics of 9N3 and 9S3 are very different, the distinctions in their complexation properties in a mixed ligand environment will be of interest. Complexes involving a second facially coordinating trithiacrown, 1,4,7-trithiacyclodecane (10S3), were also prepared. Conformational distinctions between 9S3 and 10S3 dominate the complexation behavior of these ligands towards transition metal ions. The conformation of the free 9S3 ligand has been shown to be the one in which all three sulfur atoms are *endodentate*, and thus it requires no reorganization for facial coordination to a metal center [35]. The possible conformations of the 10S3 ligand have been previously described, and only four are oriented for facial tridentate coordination. In contrast to 9S3, molecular mechanics calculations have shown that none of the lowest energy conformations of the 10S3 involve an exclusive *endodentate* conformation [36]. Employing these three macrocycles, we wish to probe how the ligand differences will influence the structural, spectroscopic, and electrochemical properties for a series of heteroleptic Cp* complexes containing Rh(III) and Ir(III).

2. Results and discussion

2.1. Syntheses

The six heteroleptic complexes are prepared by direct ligand substitution reactions from their commercially available dichloro bridged bis complexes ([{M(Cp*)$(Cl)_2$}$_2$], M = Rh or Ir) using two molar equivalents of the macrocycle and subsequently isolated as hexafluoro-

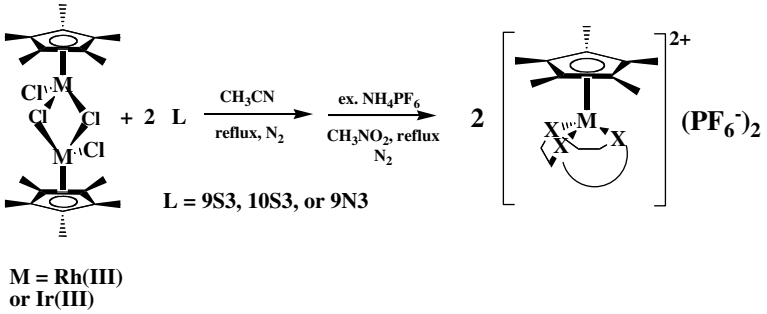

Scheme 1.

phosphate salts. These reactions are illustrated in Scheme 1. All of the complexes are highly stable both as a solid and in solution.

The presence of the Cp* and macrocyclic ligands as well as uncoordinated hexafluorophosphate is confirmed via infrared spectroscopy, and the elemental analyses are consistent with the reported complex stoichiometries. In addition, all complexes are supported by their solution ^{1}H and $^{13}C\{^{1}H\}$ NMR spectra, and five of the complex cations are characterized by single crystal X-ray diffraction as described below. The electronic spectra of the Rh(III) complexes are dominated by charge transfer transitions as typically observed in homoleptic macrocyclic complexes [27,32]. Two charge transfer bands are also seen in the electronic spectra of all Ir(III) complexes, but they also display a lower intensity long wavelength transition, assigned as a d–d transition. Again, this is consistent with observations on Ir(III) homoleptic complexes involving 9S3 and 9N3 [33,34].

The Rh(III) and Ir(III) Cp* complexes with 9S3 have been synthesized previously as perchlorate salts [22]. Our current synthetic method eliminates not only the required dechlorination by silver(I) but also the safety concerns regarding the handling of perchlorates. All three macrocycles are robust enough to displace the coordinated chlorides from the trivalent metal centers, and the insolubility in nitromethane of the ammonium chloride by-product facilitates its removal. The two reactions involving the 9N3 ligand worked better using a methanol–water mixture in the second step. Last, we would note that the metathesis from the chloride to the hexafluorophosphate salt does require some reaction time at elevated temperatures to complete fully this conversion.

2.2. Structural studies

The structures of $[Rh(\eta^5\text{-Cp*})(9S3)](Cl)_2$ (**1a**), $[Rh(\eta^5\text{-Cp*})(9N3)](PF_6)_2$ (**2**), $[Rh(\eta^5\text{-Cp*})(10S3)](PF_6)_2$ (**3**), $[Ir(\eta^5\text{-Cp*})(9S3)](PF_6)_2$ (**4**) and $[Ir(\eta^5\text{-Cp*})(9N3)](PF_6)_2$ (**5**) were determined by single-crystal X-ray diffraction. The cation in Figure **1a** was previously reported as a perchlorate salt, but limited information was presented [22]. The compound in this report crystallizes in a different space group. A crystallographic summary is given in Table 1, selected bond distances and angles in Table 2, and structural perspectives are shown in Figs. 1–5. All five structures feature facial coordination of both the η^5-Cp* ligand and the tridentate macrocycle to form a six-coordinate distorted octahedral geometry. The macrocycles have all three donor atoms orientated in an *endodentate* fashion in the complexes. The angle between the least square planes defined by the five ring carbons of the Cp* ligand and the three donor atoms of the macrocycle are all close to 0° (0.46(0.22)°–1.66(0.13)°). Similarly, the angle between the least square planes for the five ring carbons and the five methyl groups (exocyclic C–C bond) is close to

Table 1
Crystallographic data for $[Rh(Cp^*)(9S3)]Cl_2 \cdot 5H_2O$ (**1a**), $[Rh(Cp^*)(9N3)](PF_6)_2 \cdot 1.5CH_3NO_2$ (**2**), $[Rh(Cp^*)(10S3)](PF_6)_2 \cdot 2CH_3NO_2$ (**3**), $[Ir(Cp^*)(9S3)](PF_6)_2 \cdot CH_3NO_2$ (**4**), and $[Ir(Cp^*)(9N3)](PF_6)_2 \cdot 1.5CH_3NO_2$ (**5**)

	(**1a**)	(**2**)	(**3**)	(**4**)	(**5**)
Empirical formula	$C_{16}H_{37}Cl_2O_5S_3Rh$	$C_{17.50}H_{31.50}F_{12}P_2N_{4.50}O_3Rh$	$C_{19}H_{35}F_{12}P_2S_3N_2O_4Rh$	$C_{17}H_{30}F_{12}P_2NO_2S_3Ir$	$C_{17.50}H_{31.50}F_{12}P_2N_{4.50}O_3Ir$
Fw (amu)	579.45	745.82	844.52	858.74	835.11
Lattice	Triclinic	Triclinic	Monoclinic	Monoclinic	Triclinic
Space group	$P-1$	$P-1$	$P2_1/c$	$P2_1$	$P-1$
a (Å)	9.2654(17)	9.5278(17)	19.613(3)	8.8250(18)	9.5312(19)
b (Å)	9.9455(19)	9.7661(18)	15.662(2)	9.3150(19)	9.788(2)
c (Å)	13.501(3)	16.010(3)	10.2447(15)	16.999(3)	15.929(3)
α(°)	91.016(3)	72.498(5)	90	90	72.72(3)
β(°)	91.080(3)	86.419(6)	97.113(3)	101.86(3)	86.25(3)
γ(°)	109.005(3)	82.422(6)	90	90	82.65(3)
V (Å^3)	1175.7(4)	1408.0(4)	3122.8(8)	1367.5(5)	1406.7(5)
Z	2	2	4	2	2
Radiation (λ, Å)	0.71073	0.71073	0.71073	0.71073	0.71073
D_{calcd} (g cm^{-3})	1.637	1.759	1.796	2.085	1.972
μ (mm^{-1})	1.244	0.829	0.952	3.942	4.968
T (K)	193(2)	193(2)	173(2)	153(2)	173(2)
Number of reflections	10,657	12,159	28,863	18,831	20,485
Number of unique reflections	5218	6488	6168	5371	5708
R_1[a]	0.0410	0.0618	0.0718	0.0247	0.0308
wR_2[b]	0.1060	0.1522	0.1458	0.0551	0.0715
GoF	1.104	1.059	1.097	1.055	1.121

[a] $R_1 = \sum\|F_o| - |F_c\|/\sum|F_o|$.
[b] $w\ R_2 = [\sum[w(F_o^2 - F_c^2)^2]/\sum[w(F_o^2)^2]]^{1/2}$.

Table 2
Selected bond distances (Å) and angles (°) for $[Rh(Cp^*)(9S3)]Cl_2 \cdot 5H_2O$ (**1a**), $[Rh(Cp^*)(9N3)](PF_6)_2 \cdot 1.5CH_3NO_2$ (**2**), $[Rh(Cp^*)(10S3)](PF_6)_2 \cdot 2CH_3NO_2$ (**3**), $[Ir(Cp^*)(9S3)](PF_6)_2 \cdot CH_3NO_2$ (**4**), and $[Ir(Cp^*)(9N3)](PF_6)_2 \cdot 1.5CH_3NO_2$ (**5**) – M = Rh or Ir; X = S or N

	(**1a**)	(**2**)	(**3**)[a]	(**4**)	(**5**)
Distances (Å)					
$M–X_1$	2.3298(8)	2.137(3)	2.3401(16)	2.3199(13)	2.135(4)
$M–X_4$	2.3317(8)	2.131(3)	2.3332(16)	2.3216(14)	2.134(4)
$M–X_7$	2.3325(7)	2.134(4)	2.3436(17)	2.3205(11)	2.135(4)
Cp–M distances					
M–C10	2.202(3)	2.171(4)	2.180(6)	2.210(5)	2.166(4)
M–C11	2.176(3)	2.155(4)	2.188(6)	2.203(4)	2.175(4)
M–C12	2.188(3)	2.165(4)	2.191(6)	2.201(4)	2.168(4)
M–C13	2.195(3)	2.172(4)	2.196(6)	2.203(5)	2.159(4)
M–C14	2.177(3)	2.152(4)	2.212(6)	2.191(5)	2.179(4)
Angles (degrees)					
$X_1–M–X_4$	88.59(3)	80.05(14)	87.42(6)	87.95(5)	79.28(16)
$X_4–M–X_7$	88.43(2)	80.12(15)	87.29(6)	87.58(4)	79.23(15)
$X_1–M–X_7$	87.98(3)	80.27(15)	95.72(6)	87.93(6)	79.34(16)
$[\tau]$[b]	1.62(0.17)	0.46(0.22)	1.66(0.13)	0.88(24)	0.54(31)
$[\theta]$[c]	0.04(19)	0.01(19)	2.0(4)	0.20(0.26)	0.76(27)

[a] The five ring carbons for the Cp* ligand are labeled C11–C15 in this structure due to the larger cyclodecane ring in 10S3.
[b] Angles between least square planes for the 5Cp* ring carbons and the three donor atoms (N or S) in the macrocycle.
[c] Angles between least square planes for the 5Cp* ring carbons and five methyl groups (ring and exocyclic C–C bond).

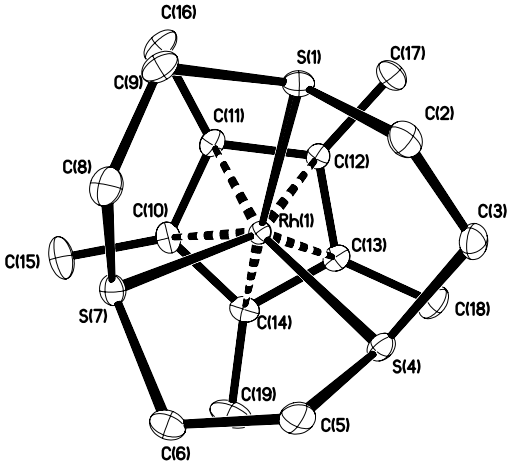

Fig. 1. Thermal ellipsoid perspective (50% probability) of cation in $[Rh(Cp^*)(9S3)]Cl_2 \cdot 5H_2O$ (**1a**).

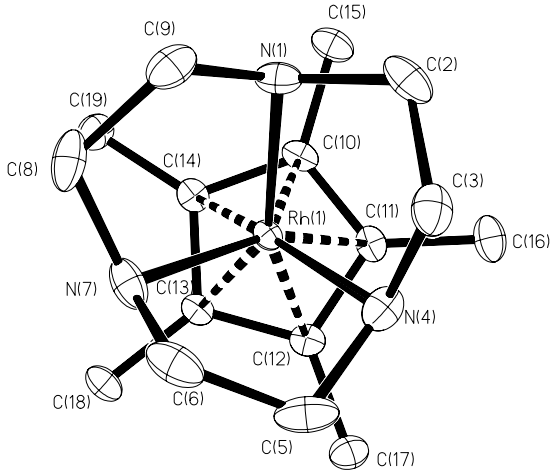

Fig. 2. Thermal ellipsoid perspective (50% probability) of cation in $[Rh(Cp^*)(9N3)](PF_6)_2 \cdot 1.5CH_3NO_2$ (**2**).

0° with the 10S3 structure showing the largest value of 2.0(4)°.

The crystal structure of $[Rh(\eta^5\text{-}Cp^*)(9S3)](Cl)_2$ (**1a**) exhibits an average Rh–S bond length of 2.3313(14) Å, an average Rh–C bond distance of 2.188(11) Å, and an average C–S bond length of 1.824(3) Å. The average S–Rh–S chelate angle is compressed to a little less than 90° at 88.3(3)°, and the 9S3 ligand adopts the [2 3 4] conformation [37]. The shorter Rh–S bond lengths in **1a** compared to the homoleptic $[Rh(9S3)_2]^{3+}$ complex (Rh–S average = 2.341(3) Å) support the π-acidity of the thioethers like 9S3 [26,27]. We propose that the strong donating ability of the Cp* enhances the π-back-bonding between the rhodium and the thioether, resulting in the Rh–S bond length changes. The rhodium center is thus better able to π donate to the thioether because of electronic affects associated with the presence of the Cp* ligand. We would also note similar structural features in a related mixed sandwich complex, $[Rh(9S3)(\kappa^3\text{-}HB(pz)_3)]^{2+}$, reported by Sheldrick [9]. This complex, too, contains short Rh–S bonds (2.293(3) Å) and long C–S bonds (1.841(3) Å). The bonding model for the heteroleptic complex is further supported by both our NMR and electrochemical data as noted below. Goh and co-workers [19] have recently reported the crystal structure of the analogous Ru(II) complex with Cp* and 9S3. The complex has an average Ru-S bond length of 2.2995(12) Å and an average Ru–C bond length of 2.195(5) Å, the former shorter and the latter

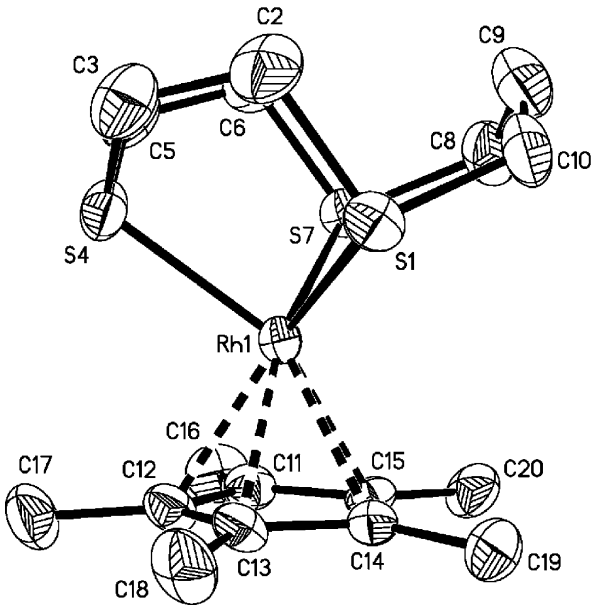

Fig. 3. Thermal ellipsoid perspective (50% probability) of cation in $[Rh(Cp^*)(10S3)](PF_6)_2 \cdot 2CH_3NO_2$ (**3**).

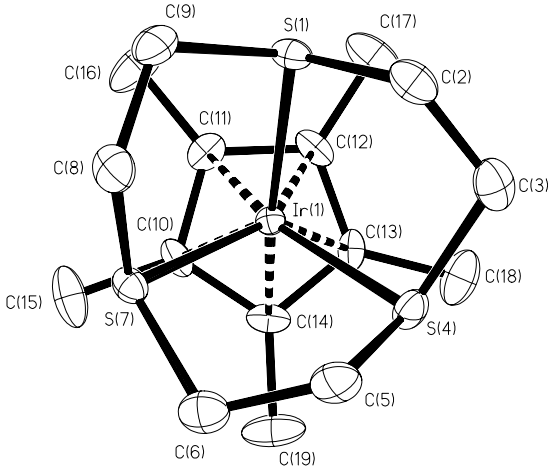

Fig. 4. Thermal ellipsoid perspective (50% probability) of cation in $[Ir(Cp^*)(9S3)](PF_6)_2 \cdot CH_3NO_2$ (**4**).

longer than in our Rh(III) complex. Given the relative charges of the two d^6 metal ions, the shorter Ru–S bond is not expected, and we believe highlights the importance of the covalency in the interaction between the metal center and the thioether.

The crystal structure of $[Rh(\eta^5\text{-}Cp^*)(9N3)](PF_6)_2$ (**2**) exhibits an average Rh–N bond length of 2.134(4) Å, an average Rh–C bond distance of 2.1639(9) Å, and an average C–N bond length of 1.495(6) Å. The N–Rh–N chelate angles are smaller, as expected, compared to the two thiacrown complexes, averaging 80.15(15)°. The Cp* ligand approaches the Rh much more closely in this complex compared to the 9S3 analog, and the 9N3 ligand adopts the [3 3 3] conformation in the structure [37]. Interestingly, the Rh–C bond distances to the Cp* ligand are shorter in this complex than in the related homoleptic metallocene, $[Rh(Cp^*)_2]^+$ (Rh–C = 2.180(5) Å) [38]. In contrast, the Rh–C distances are slightly longer in the 9S3 complex (2.188(3) Å).

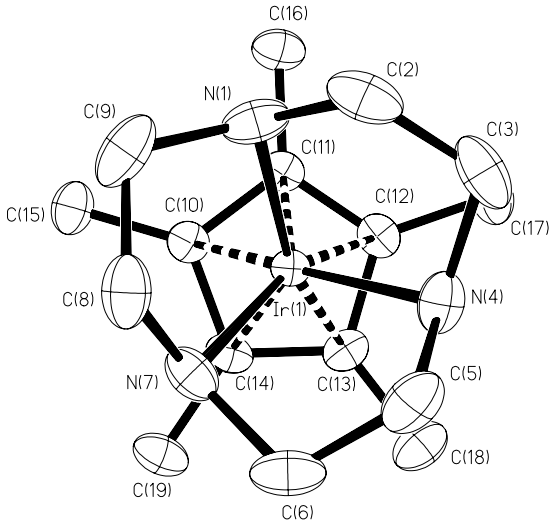

Fig. 5. Thermal ellipsoid perspective (50% probability) of cation in $[Ir(Cp^*)(9N3)](PF_6)_2 \cdot 1.5CH_3NO_2$ (**5**).

The crystal structure of $[Rh(\eta^5\text{-}Cp^*)(10S3)](PF_6)_2$ (**3**) displays an average Rh–S bond length of 2.339(5) Å. The Rh–S bond lengths are longer in this complex compared to the 9S3 analog due to the conformational differences between the two ligands. The average Rh–C distance for the Cp* ring is 2.193(12) Å, slightly longer than that observed in the 9S3 complex, and the C–S bond lengths average 1.818(14) Å. As expected, the internal S–Rh–S angles of the two five-membered chelate rings are smaller than the one containing the six-membered chelate rings (87.42(6)° and 87.29(6)° vs. 95.72(6)°) and average about a degree smaller than the five-membered chelates in the 9S3 structure. The 10S3 ligand adopts the [2 3 2 3] conformation in the crystal structure of **3**, the most common conformation seen in the crystal structures of its complexes [15,36,39]. This conformation necessarily places the six-membered chelate ring in a chair form. Viewing the cation of **3** through the 10S3 ligand, the central methylene carbon of the propylene chain is opposite the carbon that is the "point" of the Cp* ring in a staggered conformation.

For the crystal structure of $[Ir(\eta^5\text{-}Cp^*)(9S3)](PF_6)_2$ (**4**), the 9S3 ligand adopts the [3 3 3] conformation, in contrast to the [2 3 4] conformation seen in the Rh(III) analog. The complex cation has been isolated as a perchlorate salt, but a structural determination was not undertaken [22]. The structure exhibits an average Ir-S bond length of 2.3207(14) Å, an average Ir–C distance of 2.202(7) Å, and an average C–S bond length of 1.826(5) Å. The S–Ir–S chelate angle averages 87.8(2)°. The metal–sulfur distance in the Ir complex

has shortened slightly (by 0.02 Å) compared to the Rh analog, and the S–M–S chelate angle is also a compressed by about half a degree. As observed for the Rh(III) case, we again see a shorter Ir–S distance (by 0.02 Å) in the heteroleptic Cp* complex when compared to the homoleptic bis 9S3 complex [33].

The crystal structure of $[Ir(\eta^5\text{-}Cp^*)(9N3)](PF_6)_2$ (**5**) exhibits an average Ir–N bond length of 2.135(4) Å, an average Ir–C distance of 2.169(8) Å, and an average C–N bond length of 1.503(7) Å. The average N–Ir–N chelate angle is 79.28(16)°, and the 9N3 ligand adopts the [3 3 3] conformation. These metal–nitrogen and metal–carbon bond distances are both longer than in the Rh Cp* complex with 9N3. The longer Ir–N bonds (by 0.2 Å) may reflect a poorer overlap between the iridium and nitrogen orbitals. In comparing the heteroleptic Cp*/9N3 complex with the homoleptic bis 9N3 complex, the Ir–N bond distances are shorter (2.087(2) Å) and the N–Ir–N chelate angle larger (81.64(10)°) when two 9N3 ligands present. As noted previously, the 9S3 shows the opposite behavior with the longer Ir-S distance in the homoleptic complex and not in the Cp* complex. The trend in bond lengths suggests that there is not the degree of covalency in the Ir–N interaction that there is in the Ir–S interaction. As we observed in the Rh complexes, we again see shorter M–C bond distances for the heteroleptic Cp*/9N3 complex compared to the homoleptic metallocene, $[Ir(Cp^*)_2]^+$ (Ir–C = 2.186(3), 2.193(7) Å), but longer M–C distances in the 9S3 complex [40,41]. Thus, for the series of complexes involving both Rh(III) and Ir(III), the M–C bond distances in the Cp* ligand follow the trend, 9N3 < Cp* < 9S3, when these are present as the second ligand in the complex.

2.3. Spectroscopic studies

The proton and carbon-13 NMR spectra of all six complexes show the correct number of peaks, splittings, and intensities associated with the two organic components; the particular tridentate macrocyclic ligand, and the ring carbons and methyl groups of the Cp* ligand [30]. The resonances for the complexed macrocycles are shifted downfield from those in the free ligands as expected. In the proton NMR spectra, the 12 methylene protons in all complexes containing the 9N3 and 9S3 ligands appear as a pair of broad resonances with a distinguishing AA′BB′ splitting pattern (see supplemental figure for proton NMR spectra) [15]. The magnetic inequivalency of the methylene protons arises from the different orientations of the protons with respect to the metal ion. This pattern contrasts the ABCD splitting observed in homoleptic bis 9S3 complexes with Rh(III) and Ir(III) [27,33]. In the two 10S3 complexes, the methylene resonances of the thiacrown exhibit a very complex second order ^{1}H NMR spectrum but a characteristic four signal $^{13}C\{^1H\}$ NMR spectrum (2:2:2:1 ratio). All three Rh(III) complexes show a distinct doublet due to ^1J (^{103}Rh–^{13}C) coupling between the ring carbons of the Cp* ligand and the rhodium center. These couplings fall in the representative range of 4–8 Hz, further supporting η^5-Cp*–Rh(III) coordination [42,21].

There are few differences in the proton and carbon NMR spectra between the Rh(III) and Ir(III) Cp* complexes involving the same macrocycle. In contrast, there are very noticeable distinctions when comparing the 9S3 and 9N3 complexes containing the same metal ion. Both 9S3 complexes show a surprisingly large chemical dispersion for the methylene protons in their ^{1}H NMR spectra. The Rh(III) complex shows a separation of 0.42 ppm between the two sets of second order AA′BB′ multiplets while the Ir(III) complex shows a dispersion of 0.40 ppm. We have also observed similar dispersions for 9S3 protons in the isoelectronic Fe(II) and Ru(II) mixed sandwich complexes with Cp as a ligand [15]. However, as noted previously, bis 9S3 complexes do not display these dispersions. Moreover, the dispersion is much smaller in the two 9N3 complexes (0.20–0.22 ppm) (see supplemental figure for proton NMR spectra). The larger dispersion in the 9S3 complexes occurs despite their greater metal–ligand distances, suggesting its origin is indeed electronic. We believe that the distinction between the two types of cyclononane macrocycles arises from the differences in their donor/acceptor properties – specifically, the π acidity of the thioether. In thiacrowns like 9S3 the C–S σ* has been proposed as the acceptor orbital with metal t_{2g} orbitals functioning as the donor orbitals [43]. Through these acceptor orbitals, the metal–thioether π backbonding creates a larger difference for the methylene proton environments which leads to the bigger dispersion. We note the carbon–sulfur bond lengthening previously discussed in our structural studies. The dispersion of the 9N3 methylene protons seems to be constant and not specific to the Cp* complexes. That is, the degree of dispersion is fairly uniform regardless of the 9N3 complex involved. For the 9S3 complexes, the dispersion is both larger than for the 9N3 complexes and is also enhanced whenever a strong donating ligand, such as Cp or Cp*, is present in a heteroleptic environment.

As we observed for the M–C bond distances, we also see significant differences in $^{13}C\{^1H\}$ NMR chemical shifts for the Cp* carbon resonances, depending upon the identity of the second ligand in the mixed sandwich complex. When the 9S3 ligand is replaced by 9N3 in the Cp* complex, the two Rh(III) complexes show a 10.3 ppm upfield shift in the ring Cp* resonance while the two Ir(III) complexes show a 12.6 ppm upfield shift. Both 10S3 complexes show ^{13}C chemical shifts for the Cp* carbon resonance similar to the 9S3 analogs, suggesting that the large upfield shift in the 9N3 complexes is due to the type of ligand donor. Interestingly, all three Rh(III) complexes show ^{1}H and $^{13}C\{^1H\}$ NMR resonances shifted

downfield relative to the decamethylrhodocenium cation, $[Rh(Cp^*)_2]^+$ [38,41]. Particularly noteworthy is the nearly 30 ppm downfield chemical shift in the ring carbon Cp* resonance when comparing our reported $[Rh(Cp^*)(9S3)]^{2+}$ to the homoleptic decamethylrhodocenium cation. For the NMR spectra between the isoelectronic mixed sandwich Rh(III) and Ru(II) complexes with Cp* and 9S3 ligands, all proton and carbon resonances in the Rh complex are shifted downfield compared to Ru complex [19]. Lastly, we observe slight downfield shifts (by 1–3 ppm) for the methylene carbon resonances in both the Rh and Ir series when contrasting the homoleptic bis 9X3 complexes with the heteroleptic Cp* complexes (second ligand (9N3 or 9S3) is replaced by Cp*).

2.4. Electrochemical studies

The electrochemistry of the six trivalent metal complexes is dominated by a single irreversible reduction near −1.2 V vs. Fc/Fc^+ which is assigned as the +3/+2 reduction of the metal. The potential of the reduction is similar for both the Rh and Ir centers, and there is surprisingly little differentiation among the three ligands, both in the potential and in the lack of reversibility of the M(III)/M(II) couple. We have observed comparable electrochemical behavior for the ruthenium(II) Cp complexes of 9S3 and 10S3 which also show an irreversible +2/+3 couple [15]. Unfortunately, we do not see the unusual Rh(III)/Rh(II) and Rh(II)/Rh(I) electrochemistry that distinguish homoleptic complexes of trithiacrowns, in particular, their ability to stabilize rare monomeric Rh(II) species [25–27]. The replacement of a thiacrown by the strongly electron-donating Cp* destabilizes the lower Rh oxidation states, making reduction more difficult. Indeed, our observed reduction potential for the +3/+2 couple of $[Rh(Cp^*)(9S3)]^{2+}$ $(-1.24V)$ falls intermediate between those of the two homoleptic complexes, $[Rh(Cp^*)_2]^+$ (−2.02 V vs. Fc/Fc^+) and $[Rh(9S3)_2]^{3+}$ (−0.71 V vs. Fc/Fc^+) [44]. The Ir(III) homoleptic complex of 9S3, $[Ir(9S3)_2]^{3+}$, shows one irreversible reduction at −1.38 V vs. Fc/Fc^+, similar to what we observe in the two Ir(III) mixed sandwich complexes [33]. The reduction occurs at a slightly more negative potential in the bis 9S3 complex, compared to our heteroleptic Cp*/9S3 complex, again due to an effect of the electron-donating Cp* ligand. Furthermore, the potentials for both of the heteroleptic Ir(III) complexes are significantly less negative than the homoleptic $[Ir(Cp^*)_2]^+$ which shows an irreversible reduction at −2.67 V vs. Fc/Fc^+ [45].

3. Conclusions

Six heteroleptic mixed sandwich complexes containing η^5-Cp*, the Group 9 transition metal ions Rh(III) or Ir(III), and three tridentate macrocycles have been successfully synthesized directly by ligand displacement from the dichloro bridged $[\{M(Cp^*)(Cl)_2\}_2]$. All six complexes are characterized in solution via ^1H and $^{13}C\{^1H\}$ NMR spectroscopy, and five complexes were structurally characterized by single-crystal X-ray diffraction. All show a distorted octahedral geometry formed by the facially coordinating tridentate macrocyclic and the carbocyclic ligand. The 9S3 complexes displayed an AA′BB′ splitting pattern of their methylene protons with a large dispersion between the two multiplet sets. The dispersion was noticeably smaller in the 9N3 complexes. The ring carbons of the Cp* ligands are shifted by over 10 ppm upfield when comparing complexes involving azacrown to those with thiacrown ligands. The electrochemistry of the complexes is dominated by irreversible metal-centered reductions near −1.2 V vs. Fc/Fc^+, and the potential shows little effect with changes in either metal center or macrocycle. Our results are consistent with the role that the π acidity plays in thiacrown ligands, and the metal–thioether π interaction is enhanced in the presence of strongly donating ligands like Cp*.

4. Experimental

4.1. Materials

The metal reagents $\{[Rh(Cp^*)(Cl)_2]\}_2$ and $\{[Ir(Cp^*)(Cl)_2]\}_2$, the ligands 9S3, 10S3, and 9N3 and ammonium hexafluorophosphate were purchased from Aldrich Chemical Company and used as received. All solvents and other reagents were used as received.

4.2. Measurements

Analyses were performed by Atlantic Microlab, Atlanta, GA. ^1H NMR and $^{13}C\{^1H\}$ NMR spectra were obtained at 298 K on a Varian Gemini 2000 300 MHz NMR spectrometer using CD_3NO_2 for both the deuterium lock and reference. UV–vis spectra were obtained in acetonitrile using a Varian DMS 200 UV–vis spectrophotometer. Infrared spectra were obtained on a Nicolet FT-IR using dry pre-weighed KBr packets (500 mg) and an ATR accessory. A Bioanalytical Systems CV-50W Potentiostat was used for all electrochemical measurements. The supporting electrolyte was 0.100 M $(Bu)_4NBF_4$ in CH_3CN, and sample concentrations of the hexafluorophosphate salts of the complexes ranged from 1.0 to 2.2 mM. All voltammograms were recorded at a scan rate of 100 mV/s. The standard three-electrode configuration was as follows: glassy carbon or Pt disk working electrode, Pt-wire auxiliary electrode, and

Ag/Ag(I) non-aqueous pseudo-reference electrode. All potentials were internally referenced against the Fc/Fc^+ couple.

4.3. Syntheses

4.3.1. Preparation of [Rh(Cp*)(9S3)]$Cl_2 \cdot 5H_2O$ (**1a**) and [Rh(Cp*)(9S3)]$(PF_6)_2$ (**1b**)

A mixture of [{Rh(Cp*)$(Cl)_2$}$_2$] (101 mg, 0.163 mmol) and 9S3 (57.5 mg, 0.333 mmol) in acetonitrile (20 mL) was refluxed under a nitrogen atmosphere for 1 h. Upon cooling overnight. yellow crystals of the chloride salt of the complex formed. These were washed with acetone (3 × 20 mL) and ether (3 × 20 mL) to yield 110 mg (58.3%) of [Rh(Cp*)(9S3)]$Cl_2 \cdot 5H_2O$ (**1a**). A crystal of the complex suitable for X-ray analysis was obtained by ether diffusion into a nitromethane solution. The ^1H and $^{13}C\{^1H\}$ NMR spectra for the chloride salt are virtually identical to the hexafluorophosphate salt (see below). ^1H NMR (CD_3NO_2): δ, 9S3, –C*H*$_2$–, 3.75–3.65 and 3.33–3.26 (m, AA′BB′, 12H); –C*H*$_3$ 2.07 (s, 15H). $^{13}C\{^1H\}$ NMR (CD_3NO_2): δ *Cp**, 108.8 (d, 5C, $^1J_{Rh-C}$ = 4.3 Hz); *9S*3, 39.0 (s, 6C); –*CH*$_3$ 9.9 (s, 5C).

For the metathesis to the hexafluorophosphate salt of the complex cation, a mixture of [Rh(Cp*)(9S3)]$(Cl)_2$ (91.2 mg, 0.186 mmol) and NH_4PF_6 (85.7 mg, 0.526 mmol) in nitromethane (20 mL) was refluxed for 1 h under nitrogen. The yellow solution was filtered and concentrated on a rotary-evaporator to 2/3 its original volume. Ether was added drop-wise to precipitate the product that was then filtered and washed with ether (3 × 10 mL). The product was recrystallized by slow diffusion of ether into nitromethane solution and then dried at 50° C under pressure for 2 d. Yellow crystals weighing 41.2 mg (31.3%, based upon chloride salt) of pentamethylcyclopentadienide(1,4,7-trithiacyclononane) rhodium(III) hexafluorophosphate (**1b**) were obtained. Anal. Calc. for $C_{16}H_{27}F_{12}P_2RhS_3$: C, 27.13; H, 3.84. Anal. Found: C, 27.47; H, 4.11. ^1H NMR (CD_3NO_2): δ, *9S3*, –C*H*$_2$ 3.75–3.65 and 3.33–3.23 (m, AA′BB′, 12H); *Cp**, –C*H*$_3$ 2.07 (s, 15H). $^{13}C\{^1H\}$ NMR (CD_3NO_2): δ, *Cp**, 108.8 (d, 5C, $^1J_{Rh-C}$ = 4.3 Hz); *9S3*, –*CH*$_2$–, 39.0 (s, 6C); *Cp**, –*CH*$_3$ 9.9 (s, 5C). FT-IR (KBr): 3000, 2946, 1560, 1419, 1053, 917, 840 (s, PF_6^-), 736, 657, 560 cm^{-1}. The electronic absorption spectrum measured in acetonitrile showed two transitions with the first λ_{max} at 340 nm (ε = 4,100 $M^{-1}\,cm^{-1}$) and the second λ_{max} at 257 nm (ε = 29,700 $M^{-1}\,cm^{-1}$). An irreversible reduction with an E_{pc} value of −1.24 V vs. Fc/Fc^+ is observed.

4.3.2. Preparation of [Rh(Cp*)(9N3)] $(PF_6)_2$ (**2**)

A mixture of [{Rh(Cp*)$(Cl)_2$}$_2$] (79.6 mg, 0.129 mmol) and 9N3 (33.0 mg, 0.255 mmol) was refluxed in acetonitrile (20 mL) under nitrogen atmosphere for 2.5 h. Upon cooling, a yellow precipitate ([Rh(Cp*)(9N3)]$(Cl)_2$), had formed which was filtered to yield 56.8 mg of this product. The intermediate chloride salt was then dissolved in 10 mL of a 1:1 methanol/water solution, a mass of NH_4PF_6 (45.5 mg, 0.279 mmol) added, and the mixture refluxed for 1 h further. The solvent was removed by evaporation. The product was then recrystallized from nitromethane/ether to yield pentamethylcyclopentadienide(1,4,7-triazacyclononane)rhodium(III) hexafluorophosphate (75.4 mg, 45.1%) as a yellow crystalline solid. Anal. Calc. for $C_{16}H_{30}F_{12}P_2RhN_3$: C, 29.40; H, 4.60, N, 6.39. Anal. Found: C, 29.40; H, 4.34, N, 6.32. ^1H NMR, ppm (CD_3NO_2): δ, *9N3, H*, 5.68 (s, b, 3H); –*CH*$_2$, 3.29–3.03 (m, AA′BB, 12H); *Cp**, –C*H*$_3$ 1.87 (s, 15H). $^{13}C\{^1H\}$ NMR, ppm (CD_3NO_2): δ, *Cp**, 98.5 (d, 5C, $^1J_{Rh-C}$ = 4.1 Hz); *9N3*, –*CH*$_2$, 52.4 (s, 6C); *Cp**, –*CH*$_3$– 9.0 (s, 5C). The electronic absorption spectrum measured in acetonitrile showed three transitions with λ_{max}'s at 342 nm (ε = 2571 $M^{-1}\,cm^{-1}$), at 308 nm (ε = 1452 $M^{-1}\,cm^{-1}$) and at 234 nm (ε = 3504 $M^{-1}\,cm^{-1}$). FT-IR (KBr): 3327 (s, b, NH), 3125, 2974, 1452, 1098, 1047, 1025, 965, 844 (s, PF_6^-), 736, 560 cm^{-1}. An irreversible reduction with an E_{pc} value of −1.27 V vs. Fc/Fc^+ and an oxidation of this reduction product with an E_{pa} value of −0.34 V vs. Fc/Fc^+ are observed. A crystal of the complex as a monoheminitromethane solvate suitable for X-ray studies was prepared by slow diffusion of ether into a nitromethane solution.

4.3.3. Preparation of [Rh(Cp*)(10S3)]$(PF_6)_2 \cdot 2MeNO_2$ (**3**)

A mixture of [{Rh(Cp*)$(Cl)_2$}$_2$] (53.5 mg, 0.0867 mmol) and 10S3 (34.2 mg, 0.176 mmol) was refluxed in acetonitrile (20 mL) under nitrogen for 2 h. The solvent was then concentrated on a rotary evaporator to 2/3 its original volume to precipitate orange crystals of pentamethylcyclopentadienide(1,4,7-trithiacyclononane) rhodium(III) chloride (70.7 mg, 80.4%) which were collected and washed with acetone (3 × 15 mL) and air-dried. ^1H NMR (CD_3NO_2): δ, *10S3*, –C*H*$_2$ 3.87–3.11 (broad, overlapping multiplets, 14H); *Cp**, –C*H*$_3$ 2.01 (s, 15H). $^{13}C\{^1H\}$ NMR, ppm (CD_3NO_2): δ, *Cp**, 108.5 (d, 5C, $^1J_{Rh-C}$ = 6.3 Hz); 10*S*3, α-*methylene*, 39.5, 39.2, 30.2 (s, 6c); 10*S*3, β-*methylene*, 25.2 (s, 1C); *Cp**, –*CH*$_3$ 9.6 (s, 5C).

For the metathesis to the hexafluorophosphate salt, a mixture of [Rh(Cp*)(10S3)]$(Cl)_2$ (53.5 g, 0.106 mmol) and NH_4PF_6 (34.2 mg, 0.210 mmol) was refluxed in nitromethane (20 mL) under nitrogen for 2 h. The yellow solution was filtered and concentrated to 2/3 its original volume. Ether was added drop-wise to precipitate the product that was collected and washed with ether (3 × 10 mL). The product was recrystallized from nitromethane solution by slow diffusion of ether, and

dried at 50 °C under pressure for 2 days. A mass of 24 mg (31% yield from chloride salt) of pentamethylcyclopentadienide(1,4,7-trithiacyclodecane)rhodium(III) hexafluorophosphate was obtained as orange needles. ^{1}H NMR, ppm (CD_3NO_2): δ, *10S3*, –C*H*$_2$ 3.93–3.12 (broad, overlapping multiplets, 14H); *Cp**, –C*H*$_3$ 2.09 (s, 15H). ^{13}C{^{1}H} NMR, ppm (CD_3NO_2): δ, *Cp**, 108.5 (d, 5C, $^1J_{Rh-C}$ = 6.3 Hz); 10*S*3, α-*methylene*, 39.4, 39.2, 30.2 (s, 6C); 10*S*3, β-*methylene*, 25.2 (s, 1C); *Cp**, –*CH*$_3$ 9.6 (s, 5C). FT-IR (KBr): 3000, 2969, 1556, 1469, 1444, 1413, 1379, 1288, 1086, 1021, 835 (s, PF_6^-), 741, 667, 560 cm^{-1}. The electronic absorption spectrum measured in acetonitrile showed three transitions with λ_{max}'s at 340 nm (ε = 7350 M^{-1} cm^{-1}), λ_{max} 310 nm (ε = 29,700 M^{-1} cm^{-1}), and λ_{max} 260 nm (ε = 34,000 M^{-1} cm^{-1}). An irreversible reduction with an E_{pc} value of −1.22 V vs. Fc/Fc$^+$ is observed. Slow diffusion of ether into a nitromethane solution yielded yellow crystals of a nitromethane solvate which were suitable for X-ray analysis.

4.3.4. Preparation of [Ir(Cp*)(9S3)] (PF_6)$_2$ · H_2O (**4**)

A mixture of [{Ir(Cp*)(Cl)$_2$}$_2$] (55.0 mg, 0.0690 mmol) and 9S3 (24.0 mg, 0.133 mmol) was refluxed in 20 mL of nitromethane under nitrogen for 2.5 h. Upon cooling a mass of NH_4PF_6 (48.0 mg, 0.294 mmol) was added to the colorless solution, and reflux was continued for 45 additional min. The solution was cooled, forming a white precipitate of NH_4Cl. The precipitate was removed by filtration, and the solution was concentrated to 2/3 of its original volume. The solution was chilled to 5 °C and ether was added dropwise to precipitate a colorless solid which was filtered and washed with ether (3 × 10 mL). The product was re-dissolved in nitromethane, recrystallized by the slow addition of ether, and then dried at 50 °C under vacuum for 2 d. A mass of 55.0 mg (50.7% yield) of colorless crystals of pentamethylcyclopentadienide(1,4,7-trithiacyclononane)iridium(III) hexafluorophosphate monohydrate was obtained. Anal. Calc. for $C_{16}H_{29}F_{12}P_2IrS_3O$: C, 23.55; H, 3.56. Anal. Found: C, 23.64; H, 3.61. ^{1}H NMR, ppm (CD_3NO_2): δ, *9S3*, –C*H*$_2$ 3.54–3.51 and 3.12–3.08 (m, AA′BB′ 12H); *Cp**, –C*H*$_3$, 2.10 (s, 15H). ^{13}C{^{1}H} NMR, ppm (CD_3NO_2): δ, *Cp**, 102.8 (s, 5C); *9S3*, –*CH*$_2$, 39.4 (s, 6C); *Cp**, –C*H*$_3$ 9.3 (s, 5C). FT-IR (KBr): 3460 (b, H_2O), 3000, 2944, 1555, 1443, 1413, 1301, 1171, 1029, 917, 840 (s, PF_6^-), 659, 555 cm^{-1}. The electronic absorption spectrum measured in acetonitrile showed three transitions with λ_{max}'s at 340 nm (ε = 558 M^{-1} cm^{-1}), 269 nm (ε = 6760 M^{-1} cm^{-1}), and 228 nm (ε = 21,400 M^{-1} cm^{-1}). An irreversible reduction with an E_{pc} value of −1.25 V vs. Fc/Fc$^+$ is observed. Subsequent diffusion of ether into a nitromethane solution yielded X-ray quality colorless crystals of the complex as a mononitromethane solvate.

4.3.5. Preparation of [Ir(Cp*)(9N3)] (PF_6)$_2$ · 1.5 $MeNO_2$ (**5**)

A mixture of [{Ir(Cp*)(Cl)$_2$}$_2$] (51.0 mg, 0.0640 mmol) and 9N3 (15.0 mg, 0.116 mmol) was refluxed in 20 mL of nitromethane under nitrogen for 2.5 h. Upon cooling, a colorless precipitate of [Ir(Cp*)(9N3)](Cl)$_2$, formed. The precipitate was filtered to yield 42.6 mg of the chloride salt. The intermediate chloride salt was re-dissolved in 20 mL of a 1:1 (v:v) methanol/water mixture containing NH_4PF_6 (47.0 mg, 0.288 mmol) and refluxed for 1 h. The solvent was completely removed by evaporation, and the colorless solid was re-dissolved in nitromethane, recrystallized by slow diffusion of ether, and dried at 50 °C under vacuum for 2 d. Colorless crystals of pentamethylcyclopentadienide(1,4,7-triazacyclononane)iridium(III) hexafluorophosphate weighing 48.0 mg (55.4%) were recovered. ^{1}H NMR, ppm (CD_3NO_2): δ, *9N3*, *NH*, 6.21 (s, b, 3H); *9N3*, –*CH*$_2$, 3.32–3.27 and 3.14–3.09 (m, AA′BB, 12H); *Cp**, –C*H*$_3$ 1.87 (s, 15H). ^{13}C{^{1}H} NMR, ppm (CD_3NO_2): δ, *Cp**, 90.2 (s, 5C); *9N3*, –*CH*$_2$, 54.3 (s, 6C); *Cp**, –*CH*$_3$, 8.8 (s, 5C). FT-IR (KBr): 3323 (s, b, NH), 3107 (s, b), 2926, 1616, 1456, 1392, 1267, 1154, 1111, 1051, 1025, 973, 840 (s, PF_6^-), 736, 666, 555 cm^{-1}. The electronic absorption spectrum measured in acetonitrile showed three transitions with λ_{max}'s at 350 nm (shoulder, ε = 300 M^{-1} cm^{-1}), at 340 nm (ε = 2571 M^{-1} cm^{-1}), at 308 nm (ε = 1452 M^{-1} cm^{-1}) and at 267 nm (ε = 2315 M^{-1} cm^{-1}). An irreversible reduction with an E_{pc} value of −1.26 V vs. Fc/Fc$^+$ is observed. Ether diffusion into a nitromethane solution yielded X-ray quality colorless crystals as a nitromethane solvate.

4.3.6. Preparation of [Ir(Cp*)(10S3)] (PF_6)$_2$ · 3$MeCN$ (**6**)

A mixture of [{Ir(Cp*)(Cl)$_2$}$_2$] (67.1 mg, 0.0842 mmol) and 10S3 (32.7 mg, 0.168 mmol) was refluxed in acetonitrile (20 mL) for 5 h under nitrogen. A pale yellow solid was collected and washed with acetone (3 × 15 mL) to yield 73.8 mg (75.5%) of pentamethylcyclopentadienide(1,4,7-trithiacyclodecane)iridium(III)chloride. For the metathesis to the hexafluorophosphate salt, a mixture of [Ir(Cp*)(10S3)](Cl)$_2$ (31.7 mg, 0.0535 mmol) and NH_4 PF_6 (17.0 mg, 0.104 mmol) was refluxed in 20 mL of nitromethane under a nitrogen atmosphere for 1 h. The pale yellow solution was filtered and then concentrated on a rotary-evaporator to 2/3 its original volume. Ether was added drop-wise to precipitate the product that was collected by filtration and washed with ether (3 × 10 mL). The product was recrystallized from acetonitrile solution by slow diffusion of ether, and dried at 50 °C under vacuum for 2 d. A mass of 10 mg (20% yield from chloride salt) of colorless crystals of [Ir(Cp*)(10S3)](PF_6)$_2$ were recovered as an acetonitrile solvate. Anal. Calc. for $C_{23}H_{38}F_{12}P_2IrS_3N_3$: C, 29.55; H, 4.10. Anal. Found: C, 29.57; H, 4.28. ^{1}H

NMR (CD_3NO_2): δ, *10S3*, $-CH_2$, 3.78–3.02 (broad, overlapping multiplets, 14H); *Cp**, $-CH_3$, 2.09 (s, 15H). $^{13}C\{^1H\}$ NMR (CD_3NO_2): δ, *Cp**, 102.7 (s, 5C), *10S3*, α-*methylene*, 39.9, 39.7, 29.5 (s, 6C); *10S3*, β-*methylene*, 25.9 (s, 1C); *Cp**, $-CH_3$ 9.6 (s, 5C). FT-IR (KBr): 2969, 2900, 1650, 1615, 1465, 1417, 1297, 1090, 1038, 840 (s, PF_6^-), 736, 660, 521 cm^{-1}. The electronic absorption spectrum measured in acetonitrile showed three transitions with the first λ_{max} at 340 nm ($\varepsilon = 980\ M^{-1}\,cm^{-1}$), the second λ_{max} at 268 nm ($\varepsilon = 7811\ M^{-1}\,cm^{-1}$), and the third λ_{max} at 230 nm ($\varepsilon = 19{,}222\ M^{-1}\,cm^{-1}$).

4.4. Data collection and processing

Suitable crystals of all complexes were grown by slow diffusion (multiday) of ether into a nitromethane solution at ambient temperatures, and a summary of key crystallographic details for all structures is presented in Table 1. Table 2 includes selected bond distances and angles for the five structures.

For the three rhodium complexes, the one with 9S3 crystallizes as a pentahydrate, the 9N3 with 1.5 molecules of nitromethane solvate per complex, and the 10S3 complex with two nitromethane solvates per complex. For the 9S3 and 9N3 structures, intensity data were collected at low temperature on a Siemens SMART 1K CCD diffractometer equipped with graphite-monochromated Mo Kα radiation ($\lambda = 0.71073$ Å) [46,47]. The structures were solved using direct methods [46], and refinement was done using full-matrix least-squares techniques (on F^2). Structure solution, refinement and the calculation of derived results were performed with the SHELXTL [47] package of computer programs. For the 10S3 structure, intensity data were measured at low temperature with graphite-monochromated Mo Kα radiation ($\lambda = 0.71073$ Å) on a Rigaku AFC7R diffractometer. Data was corrected for Lorentz and polarization effects and for absorption, using semi-empirical methods. The structure of the 10S3 complex was solved by direct methods and refined by using full-matrix least-squares techniques (on F^2). All non-hydrogen atoms were refined anisotropically; hydrogen atoms were placed in optimized positions ($d_{C-H} = 0.96$ Å) with assigned thermal parameters equal to 120% of the U_{eq} value of their host atom. Structure solution, refinement and the calculation of derived results were performed with the SHELXTL package of computer programs [48]. Neutral atom scattering factors were those of Cromer and Waber [49], and the real and imaginary anomalous dispersion corrections were those of Cromer [49]. For the two Ir(III) structures, the 9S3 complex crystallizes as a mononitromethane solvate while the 9N3 complex crystallizes with 1.5 molecules of nitromethane per complex. The intensity data for these were measured at low temperature with graphite-monochromated Mo Kα radiation ($\lambda = 0.71073$ Å) on a Rigaku AFC8S diffractometer equipped with a 1 K mercury CCD detector [50,51]. Structure solution, refinement and the calculation of derived results were performed with the SHELXTL package of computer programs [48].

Acknowledgements

This research was generously supported by grants from Merck/AAAS, the Petroleum Research Fund of the American Chemical Society, the Camille and Henry Dreyfus Foundation (to M.L.H.), the National Science Foundation RSEC Program at UT-Knoxville (L.F.M. and D.W.K.), and the Grote Chemistry Fund at UTC.

Appendix A. Supplementary data

Crystallographic data for the five structures reported in this paper have been deposited with the Cambridge Crystallographic Data Centre as CCDC 246944–246948. Copies of the data can be obtained free of charge upon application to CCDC, 12 Union Road, Cambridge, CB2 1 EZ UK (Fax: +44 1223 336 033); e-mail: deposit@ccdc.cam.ac.uk. Proton and carbon-13 NMR spectra for $[Rh(Cp^*)(9S3)](PF_6)_2$ and $[Rh(Cp^*)(9N3)](PF_6)_2$ are available. Supplementary data associated with this article can be found, in the online version at doi:10.1016/j.jorganchem.2004.10.010.

References

[1] P. Chaudhuri, K. WieghardtProgress in Inorganic Chemistry, vol. 35, Wiley, New York, 1987, p. 329.
[2] A.J. Blake, M. Schröder, in: A.G. Sykes (Ed.), Advances in Inorganic Chemistry, vol. 35, Academic Press, New York, 1990, p. 2.
[3] S.R. Cooper, S.C. Rawle, Struct. Bond. (Berlin) 72 (1990) 1.
[4] R.D. Adams, S.B. Falloon, K.T. McBride, J.H. Yamamoto, Organometallics 14 (1995) 1748.
[5] R.D. Adams, K.M. Brosius, O.-S. Kwon, J. Organomet. Chem. 652 (2002) 51.
[6] M.A. Bennett, L.Y. Goh, A.C. Willis, J. Am. Chem. Soc. 118 (1996) 4984.
[7] M.A. Bennett, A.C. Willis, L.Y. Goh, W. Chen, Polyhedron 15 (1996) 3559.
[8] A.J. Welch, A.S. Weller, Inorg. Chem. 35 (1996) 4548.
[9] K. Brandt, W.S. Sheldrick, J. Chem. Soc., Dalton Trans. (1996) 1237.
[10] J. Cannadine, A. Hector, A.F. Hill, Organometallics 11 (1992) 2333.
[11] A.F. Hill, J.D.E.T. Wilton-Ely, Organometallics 16 (1997) 4517.
[12] J. Cannadine, A.F. Hill, A.J.P. White, D.J. Williams, J.D.E.T. Wilton-Ely, Organometallics 15 (1996) 5409.
[13] A.J. Blake, M.A. Halcrow, M. Schröder, J. Chem. Soc., Chem. Commun. (1991) 253.
[14] A.J. Blake, M.A. Halcrow, M. Schröder, J. Chem. Soc., Dalton Trans. (1994) 1631.

[15] G.J. Grant, T. Salupo-Bryant, L.A. Holt, D.Y. Morrissey, M.J. Gray, J.D. Zubkowski, E.J. Valente, L.F. Mehne, J. Organomet. Chem. 587 (1999) 207.
[16] A.J. Blake, R.D. Crofts, G. Reid, M. Schröder, J. Organomet. Chem. 359 (1989) 371.
[17] M. Green, M. Draganjac, Y. Jiang, A.W. Cordes, J. Chem. Cryst. 29 (1999) 273.
[18] R.Y.C. Shin, M.A. Bennett, L.Y. Goh, W. Chen, D.C.R. Hockless, W.K. Long, K. Mashima, A.C. Willis, Inorg. Chem. 42 (2003) 96.
[19] L.Y. Goh, M.E. Teo, S.B. Khoo, W.K. Leong, J.J. Vittal, J. Organomet. Chem. 664 (2002) 161.
[20] D.L. Davies, J. Fawcett, S.A. Garratt, D.R. Russell, J. Organomet. Chem. 662 (2002) 43.
[21] E. Carmona, A. Cingolani, F. Marchetti, C. Pettinari, R. Pettinari, B.W. Skelton, A.H. White, Organometallics 22 (2003) 2820.
[22] H.J. Kim, J.H. Jeong, Y. Do, Bull. Kor. Chem. Soc. 13 (1992) 463.
[23] S.R. Klei, J.T. Golden, D.T. Tilley, R.G. Bergman, J. Am. Chem. Soc. 124 (2002) 2092.
[24] B.A. Arndtsten, R.G. Bergman, T.A. Mobley, T.H. Peterson, Acc. Chem. Res. 28 (1995) 154.
[25] S.R. Cooper, S.C. Rawle, R. Yagbasan, D.J. Watkin, J. Am. Chem. Soc. 113 (1991) 1600.
[26] S.C. Rawle, R. Yagbasan, K. Prout, S.R. Cooper, J. Am. Chem. Soc. 109 (1987) 6181.
[27] A.J. Blake, R.O. Gould, A.J. Holder, T.I. Hyde, M. Schröder, J. Chem. Soc. Dalton Trans. (1988) 1861.
[28] H.-J. Kim, J.-H. Lee, I.-H. Suh, Y. Do, Inorg. Chem. 34 (1995) 796.
[29] A.J. Blake, A.J. Holder, T.I. Hyde, H.-J. Küppers, M. Schröder, S. Stozel, K. Wieghardt, J. Chem. Soc., Chem. Commun. (1989) 1600.
[30] M.N. Bell, A.J. Blake, M. Schröder, T.A. Stephenson J. Chem. Soc., Chem. Commun. (1986), 471. The authors report that the Rh(III) complexes of 9N3 and 9S3 have been characterized by NMR, but no details were given in the paper.
[31] M. Sudfield, W.S. Sheldrick, Inorg. Chim. Acta 304 (2000) 78.
[32] F. Galsból, C.H. Petersen, K. Simonsen, Acta Chem. Scand. 50 (1996) 567.
[33] A.J. Blake, R.O. Gould, A.J. Holder, T.I. Hyde, G. Reid, M. Schröder, J. Chem. Soc. Dalton Trans. (1990) 1759.
[34] C. Flensburg, K. Simonsen, L.K. Skov, Acta Chem. Scand. 48 (1994) 209.
[35] R.S. Glass, G.S. Wilson, W.N. Setzer, J. Am., Chem. Soc. 102 (1980) 5068.
[36] W.N. Setzer, E.L. Cacioppo, Q. Guo, G.J. Grant, D.D. Kim, J.L. Hubbard, D.G. VanDerveer, Inorg. Chem. 29 (1990) 2672.
[37] J. Dale, Acta Chem. Scand. 27 (1973) 1115.
[38] D. Buchholz, L. Zsolnai, G. Huttner, D. Astruc, J. Organomet. Chem. 593-594 (2000) 494.
[39] G.J. Grant, B.M. McCosar, W.N. Setzer, J.D. Zubkowski, E.J. Valente, L.F. Mehne, Inorg. Chim. Acta 244 (1996) 73.
[40] Y.T. Struckhov, M. Yu, K.A. Lyssenlo, O.V. Gusev, T.A. Peganova, N.A. Ustynuk, J. Organomet. Chem. 536-537 (1997) 281.
[41] Y. Zhang, Z. Hou, Y. Wakatsuki, Bull. Chem. Soc. Jpn 71 (1998) 1381.
[42] J. Ruiz, B.E. Mann, C.M. Spencer, B.F. Taylor, P.M. Maitlis, J. Chem. Soc. Dalton Trans. (1987) 1963;
B.E. Mann, B.F. Taylor, ^{13}C NMR Data for Organometallic Compounds, Academic Press, London, 1981, pp. 239-241.
[43] G.E.D. Mullen, T.F. Fässler, M.J. Went, K. Holand, B. Stein, P.J. Blower, J. Chem. Soc. Dalton Trans. (1999) 3759.
[44] U. Kölle, W. Kläui, Z. Naturforsch. 46b (1991) 75.
[45] O.V. Gusev, M.G. Peterleitner, M.A. Ievlev, A.M. Kal'sin, P.V. Petrovskii, L.I. Denisovich, N.A. Ustynyuk, J. Organomet. Chem. 531 (1997) 95, The electrochemical reduction of $[Ir(Cp^*)_2]^+$ leads to the formation of a ligand-bridged dimer. The large difference in potentials between this complex and the two Ir complexes in our report suggests that we are indeed observing metal-centered reductions.
[46] The programs used for data collection, solution and refinement of this structure were: SMART 5.054, SAINT$^+$ 6.01, SHELXTL 5.1, 1998–1999, Bruker AXS, Madison, WI, USA.
[47] SADABS R.H. Blessing, Acta Cryst. A 51 (1995) 33.
[48] SHELXTL 5.1, 1998–1999, Bruker AXS, Madison, WI, USA.
[49] D.T. Cromer, J.T. Waber, International Tables for X-ray CrystallographyTable 2.2B, vol. IV, The Kynoch Press, Birmingham, England, 1974;
D.T. Cromer, International Tables for X-ray CrystallographyTable 2.3.1, vol. IV, The Kynoch Press, Birmingham, England, 1974.
[50] CrystalClear; Rigaku/MSC, The Woodlands, TX, USA, 1999.
[51] R.A. Jacobson, REQAB subroutine of CrystalClear, Rigaku/MSC, The Woodlands, TX, USA, 1999.